

# Use of Fast Protein Size-Exclusion Liquid Chromatography To Study the Unfolding of Proteins Which Denature through the Molten Globule†

Vladimir N. Uversky

*Institute of Protein Research, Russian Academy of Sciences, 142292 Pushchino, Moscow Region, Russia*

*Received June 10, 1993; Revised Manuscript Received August 30, 1993\**

**ABSTRACT:** Fast protein size-exclusion liquid chromatography (SEC-FPLC) was used to study solvent-induced unfolding of six proteins. Two of them (sperm whale myoglobin and hen white lysozyme) denature on the simple N (native)  $\rightleftharpoons$  U (completely unfolded) scheme. The other four proteins [bovine and human  $\alpha$ -lactalbumin, bovine carbonic anhydrase B (BCAB), and  $\beta$ -lactamase from *Staphylococcus aureus*] denature through the molten globule (MG) state (i.e., on the N  $\rightleftharpoons$  MG  $\rightleftharpoons$  U denaturation scheme). We have shown that the permeation properties of the Superose 12 columns are practically independent of temperature, pH, and denaturants in wide concentration intervals. In the case of myoglobin and lysozyme denaturation at 4 °C (when the exchange between the native and unfolded states is slower than the characteristic time of chromatography), a bimodal distribution on molecular dimensions in the transition region was observed. This indicates that, under denaturant action, protein molecules can only be in one of the two states with different compactness. In other words, this shows that FPLC is one of the most direct approaches to establish the “all-or-none” mechanism of the equilibrium solvent-induced denaturation of globular proteins. The curves of guanidinium hydrochloride- (GdmHCl) or urea-induced unfolding (N  $\rightleftharpoons$  U or MG  $\rightleftharpoons$  U transitions) of a protein on a column (monitored either by the relative areas of two peaks or—for fast exchange—by the position of the average peak) coincide with those monitored by far-UV CD in solution. The Stokes radius values obtained with the use of FPLC for the molten globule states of BCAB (1.6 M GdmHCl in 0.1 M sodium phosphate, pH 6.8, and acid form at pH 3.6) and for the human  $\alpha$ -lactalbumin molten globule (2.0 M GdmHCl in 0.1 M sodium phosphate, pH 6.8) coincide with those known from literature. Thus, it has been shown that fast protein size-exclusion liquid chromatography (FPLC) is an “inert” technique, i.e., it does not shift the equilibrium between N, MG, and U states and, therefore, can be used for qualitative and quantitative studies of protein denaturation.

It is well-known that the studies of thermal or solvent-induced denaturation of protein molecules are very useful for the understanding of protein folding pathways (Tanford, 1968, 1970; Wong & Tanford, 1973; Privalov, 1979). As strong changes of many protein properties (including the large changes of molecular dimensions) associate with these processes, a wide variety of physicochemical techniques are used for the studies of the protein denaturation. As was already mentioned by Corbett and Roche (1984), while one of the most theoretically well-founded methods for determining volume changes is intrinsic viscosity, gel filtration techniques offer an alternative approach, which is based on the existence of the good correlation between the retention time measured by the gel filtration column and the Stokes radius of the protein molecule (Ackers, 1967, 1970; Corbett & Roche, 1984).

When the exchange between conformers in the transition region is slower than the characteristic time of chromatography, it is possible to show that the function of their distribution on a dimension is *bimodal*. This indicates that the solvent-induced unfolding of small globular proteins is really of the “all-or-none” character. What is more, in this case we have an exceptional possibility to record changes of dimensions of both the native and unfolded molecules simultaneously.

The ability of chromatography to detect conformational differences between proteins is a new area of investigation—the first attempts to use analytical gel filtration for studies of

protein denaturation in various solvents were made by Tanford and co-workers (Fish *et al.*, 1970). Conformational changes in several proteins have been detected by size-exclusion chromatography (SEC)<sup>1</sup> in terms of changes in retention time, which correlates with the changes of Stokes radii of the protein conformers (Corbett & Roche, 1983, 1984; Endo *et al.*, 1983; Lau *et al.*, 1984; Brems *et al.*, 1985) or as the appearance of a new peak (Calam & Davidson, 1981; Endo *et al.*, 1983; Gupta, 1983; Ingham *et al.*, 1983; Corbett & Roche, 1983, 1984; Houghlum & Chappel, 1984; Withka *et al.*, 1987; Uversky *et al.*, 1992).

Proteins (see above), whose unfolding was studied by size-exclusion chromatography, denatured usually in a two-state manner (i.e., according to the simple N  $\rightleftharpoons$  U scheme). It has been determined that neither N nor U states interact with the column matrix; i.e., a column does not shift the equilibrium between these conformers [see, for example, Corbett and Roche (1984)]. The question arises: Is it correct to use SEC for the studies of the unfolding proteins that denature through the molten globule state (i.e., on the N  $\rightleftharpoons$  MG  $\rightleftharpoons$  U denaturation scheme) because the column can probably affect this intermediate. In this paper, we show that SEC-FPLC is an “inert” technique, i.e., it does not shift the equilibrium between the N, MG, and U states and, therefore, can be used for a quantitative study of protein denaturation. In particular, the

† This study was supported in part by the Russian Foundation for Fundamental Investigations (Grant No. 93-04-6635).

\* Abstract published in *Advance ACS Abstracts*, October 15, 1993.

<sup>1</sup> Abbreviations: N (native), MG (molten globule), and U, completely unfolded states of a protein molecule; CD, circular dichroism; UV, ultraviolet; GdmHCl, guanidinium hydrochloride; SEC, size exclusion chromatography;  $R_s$ , Stokes radius; MW, molecular weight;  $V_{el}$ , elution volume; BCAB, bovine carbonic anhydrase B; BSA, bovine serum albumin; LDH, lactate dehydrogenase.

Table I: Stokes Radii ( $R_S$ ) for Proteins in Native State and Completely Unfolded by GdmHCl (without Cross-Links)<sup>a</sup>

protein	native state		Unfolded state		reference
	mol wt	$R_S^N$ (Å)	mol wt	$R_S^U$ (Å)	
insulin*	5 780	13.6 <sup>b</sup>	2 970	14.2 14.8 <sup>b</sup>	Tanford <i>et al.</i> (1967)
ubiquitin*	8 500	15.7 <sup>b</sup>	8 500	25.8 <sup>b</sup>	Tanford (1970)
cytochrome <i>c</i> *	11 700	17.0	11 700	30.4	
ribonuclease*	13 700	17.6 <sup>b</sup>	13 700	30.6 <sup>b</sup>	Tanford <i>et al.</i> (1967)
		19.3		32.8	
		19.7 <sup>b</sup>		33.3 <sup>b</sup>	
lysozyme*	14 300	20.2 <sup>d</sup>	14 300	29.3 <sup>c,d</sup>	Tanford (1968)
		20.0 <sup>b</sup>		33.8	
				34.1 <sup>b</sup>	
hemoglobin	64 500	33.2	15 500	35.9	Tanford <i>et al.</i> (1967)
myoglobin*	16 900	35.1 <sup>b</sup>	16 900	35.6 <sup>b</sup>	Tanford <i>et al.</i> (1967)
		20.2		37.8	
$\beta$ -lactoglobulin*	36 800	21.3 <sup>b</sup>	18 400	37.3 <sup>b</sup>	Tanford <i>et al.</i> (1967)
		27.1		40.5	
chymotrypsinogen*	25 700	28.5 <sup>b</sup>	25 700	39.0 <sup>b</sup>	Tanford <i>et al.</i> (1967)
		21.7		47.8	
carbonic anhydrase*	28 800	23.9 <sup>b</sup>	28 800	46.6 <sup>b</sup>	Wong & Tanford (1973)
		23.6		51.3	
		24.4 <sup>b</sup>		49.5 <sup>b</sup>	
<i>S. aureus</i> $\beta$ -lactamase*	30 000	24.2 <sup>b</sup>	30 000	49.9 <sup>b</sup>	Voll <i>et al.</i> (1967)
phosphoribosyl transferase	210 000	51.0 <sup>b</sup>	35 000	56.1	
				55.1 <sup>b</sup>	
LDH	141 000	43.9 <sup>f</sup>	35 000	56.2 <sup>g</sup>	<i>f</i>
		44.3 <sup>c</sup>		55.1 <sup>c</sup>	<i>g</i>
glyceraldehyde-3-phosphate dehydrogenase	145 000	44.3	36 300	58.3	Harrington & Karr (1965)
		44.7 <sup>b</sup>		56.0 <sup>c</sup>	
pepsinogen	40 000	27.3	40 000	58.4	Tanford <i>et al.</i> (1967)
		27.8 <sup>b</sup>		59.0 <sup>c</sup>	
ovalbumin*	43 500	30.2	43 500	52.0	Castellino & Barker (1968)
		28.7 <sup>b</sup>		61.7 <sup>c</sup>	
aldolase*	160 000	46.6	40 000	60.8	Tanford <i>et al.</i> (1967)
		46.4 <sup>b</sup>		59.0 <sup>c</sup>	
BSA*	66 300	33.9	66 300	81.8	Tanford <i>et al.</i> (1967)
		33.5 <sup>b</sup>		77.3 <sup>c</sup>	
transferrin	81 000	36.0 <sup>h</sup>	81 000	86.8 <sup>i</sup>	<i>h</i>
		36.1 <sup>b</sup>		86.0 <sup>c</sup>	<i>i</i>
tyroglobulin	660 000	78.8	165 000	128.8	DeCrombrugghe <i>et al.</i> (1966)
		78.2 <sup>b</sup>		125.6 <sup>c</sup>	
catalase*	220 000	52.0			LeMaire <i>et al.</i> (1980)
		52.2 <sup>b</sup>			
ferritin*	450 000	67.9 <sup>b</sup>			

<sup>a</sup> The  $R_S$  values of proteins whose intrinsic viscosity ( $[\eta]$ ) is known from literature were calculated using the relationship proposed by Tanford (1970):  $[\eta] = (2.5 N_A/MW) (4/3 \pi R_S^3)$ , where  $N_A$  is Avogadro's number and MW is the protein molecular weight. (\*) indicates the proteins which were used for calibration of the Superose-12 column. <sup>b</sup>  $R_S$  were calculated from the equation:  $\log(R_S) = 0.369 \log(MW) - 0.254$ . <sup>c</sup>  $R_S$  were calculated from the equation:  $\log(R_S) = 0.533 \log(MW) - 0.682$ . <sup>d</sup>  $R_S$  values for lysozyme were determined using dynamic light scattering (Gast *et al.*, 1991). <sup>e</sup>  $R_S$  value for unfolded lysozyme with oxidised disulfide bridges. <sup>f</sup> Castellino & Barker (1968). <sup>g</sup> Corbett & Roche (1984). <sup>h</sup> LeMaire *et al.* (1980). <sup>i</sup> Fish *et al.* (1970).

results of the application of SEC-FPLC to the quantification of the molecular dimension changes upon the equilibrium unfolding of bovine and human  $\alpha$ -lactalbumins, bovine carbonic anhydrase B, and  $\beta$ -lactamase from *Staphylococcus aureus* (which denature according to the N  $\rightleftharpoons$  MG  $\rightleftharpoons$  U scheme) in comparison with the changes of their far-UV CD are presented. Moreover, the Stokes radii obtained by FPLC for the molten globule states of BCAB (1.6 M GdmHCl in 0.1 M sodium phosphate, pH 6.8, and the acid form at pH 3.6) and for the human  $\alpha$ -lactalbumin molten globule (2.0 M GdmHCl in 0.1 M sodium phosphate, pH 6.8) coincide with literature data.

## MATERIALS AND METHODS

**Solution Preparation and Handling.** Carbonic anhydrase B was purified from bovine blood erythrocytes by N. V. Kotova (Institute of Protein Research).  $\beta$ -Lactamase was purified from *Staphylococcus aureus* by T. Picard (University of Newcastle-upon-Tyne).  $\alpha$ -Lactalbumins (from bovine and

human milk) and bovine milk  $\beta$ -lactoglobulin were purified by V. E. Bychkova and N. V. Kotova (Institute of Protein Research). Lysozyme (hen egg white) was from Boehringer Mannheim GmbH (Vienna, Austria). Whale skeletal muscle myoglobin was from Sigma (Sigma type 11).

The following proteins were used for column calibration under a variety of conditions: thyroglobulin (Pharmacia AB, gel filtration calibration kit); ferritin, catalase, aldolase, bovine serum albumin, ovalbumin from hen egg, chymotrypsinogen A, and cytochrome *c* (calibration proteins 1 for gel chromatography, Combithek, Boehringer Mannheim GmbH). Blue dextran (Sigma) and acetone were also used in column calibration.

All solutions prepared for FPLC were passed through a 0.2- $\mu$ m nylon 66 filter (Rainin Instrument Co.).

The concentrations of proteins in solutions were determined spectrophotometrically. Esterase activity of BCAB was measured by the rate of increase of absorption at 348 nm, which is the measure of *p*-nitrophenylacetate (Sigma) cleavage

Table II: Stokes Radii ( $R_S$ ) for Proteins without Cross-Links Completely Unfolded by Urea<sup>a</sup>

protein	mol wt (Da)	$R_S^U$ (Å)	reference
insulin	2 970	14.6*	
ribonuclease	13 700	32.4	Lapanje (1969)
		32.4	
lysozyme	14 300	33.0	Tanford (1968)
		33.1	
$\beta$ -lactaglobulin	18 400	39.8	Lapanje (1969)
		37.8	
chymotrypsinogen	25 700	45.0	Tanford (1968)
		45.1	
BCAB	28 800	50.1	Rodionova <i>et al.</i> (1989)
		47.8	
$\beta$ -lactamase	30 000	48.9*	
ovalbumin	43 500	58.8	Ahmad & Salahuddin (1974)
		59.4	
BSA	66 300	76.8	Lapanje (1969)
		74.0*	

<sup>a</sup>  $R_S$  values were calculated from intrinsic viscosity ( $[\eta]$ ) data. (\*) indicates the  $R_S$  values which were calculated from the equation:  $\log(R_S) = 0.524 \log(MW) - 0.657$ .

(Armstrong *et al.*, 1966). Enzymatic activity of  $\beta$ -lactamase was measured by the rate of decrease of absorption at 235 nm, which is the measure of penicillin-G (Sigma) cleavage (Janson, 1965).

Measurements were made at 23, 15, and 4 °C. In the latter case, the solutions were preincubated for 40 h at 4 °C.

Urea and guanidinium hydrochloride (GdmHCl) were purified by recrystallization from water and from ethanol, respectively. The denatured concentration in solution was measured by the refractive index.

To avoid the influence of protein association on the results of SEC-FPLC measurements, the usual protein concentration was about 0.001 mg/mL.

**Equipment.** In size-exclusion chromatography experiments, we used the Superose-12 column and FPLC equipment (Pharmacia, Uppsala, Sweden). To study very diluted protein solutions, 2158 Uvicord SD (LKB) was equipped with the 226-nm filter. SEC measurements at 4 °C were made in a cold room. Circular dichroism was measured with a Jasco-600 spectropolarimeter (Japan Spectroscopic Co., Ltd., Tokyo). Enzymatic activities were determined with a Specord M40 spectrophotometer (Carlzeiss, Jena, Germany). Fluorescent measurements were made with an Aminco (SPF-1000CS) corrected spectrofluorimeter (American Instrument Corporation, Silver Spring, MD). All these spectral instruments were equipped with a temperature-controlled holder.

**Determination of Stokes Radii for Native and Unfolded Proteins.** Stokes radii of native and completely unfolded proteins of known molecular weight were determined according to the following procedure. At the first step, the set of proteins whose molecular weights and Stokes radii in the native and/or completely unfolded states are known from literature (see Tables I and II) was used to construct the calibration curves [the dependences of  $\log(R_S)$  vs  $\log(MW)$ ] for the native and GdmHCl- or urea-unfolded proteins (see Figure 1). Such a dependence for the native proteins is described by

$$\log(R_S) = -(0.254 \pm 0.002) + (0.369 \pm 0.001) \log(MW) \quad (1)$$

For proteins unfolded by GdmHCl:

$$\log(R_S) = -(0.543 \pm 0.004) + (0.502 \pm 0.001) \log(MW) \quad (2)$$

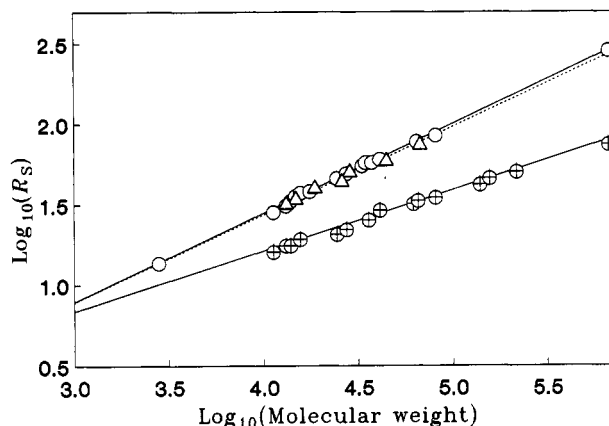


FIGURE 1: Dependences of  $\log(R_S)$  on  $\log(MW)$  for native (●) and completely unfolded by GdmHCl (○) or urea (Δ) proteins without cross-links. Data for these dependences were taken from the literature (see Tables I and II).

Table III: Comparison of Superose-12 Column Permeation Properties under Various Experimental Conditions

exptl conditions (solvent system and temperature)	void vol, $V_0$ (mL) <sup>a</sup>	total solvent-accessible vol, $V_t$ (mL) <sup>b</sup>
0.1 M sodium phosphate, pH 6.8, 23 °C	7.45	19.38
0.1 M sodium phosphate, pH 6.8, 15 °C	7.49	19.41
0.1 M sodium phosphate, pH 6.8, 4 °C	7.46	19.45
0.1 M sodium phosphate, pH 3.6, 23 °C	7.51	19.44
0.1 M sodium phosphate, 6.0 M GdmHCl, pH 6.8, 23 °C	7.56	19.46
0.1 M sodium phosphate, 6.0 M GdmHCl, 0.01 M DTT, pH 6.8, 23 °C	7.53	19.42
0.1 M sodium phosphate, 6.0 M GdmHCl, pH 6.8, 15 °C	7.52	19.47
0.1 M sodium phosphate, 6.0 M GdmHCl, pH 6.8, 4 °C	7.48	19.42
0.1 M sodium phosphate, 8.0 M urea, 0.01 M DTT, pH 6.8, 23 °C	7.55	19.40
0.1 M sodium phosphate, 8.0 M urea, pH 6.8, 4 °C	7.49	19.44

<sup>a</sup> The value of the column void volume is based on the elution volume of blue dextran. <sup>b</sup> The value of the total solvent-accessible column volume is based on the elution volume of acetone.

In the case of urea-induced unfolding:

$$\log(R_S) = -(0.657 \pm 0.04) + (0.524 \pm 0.001) \log(MW) \quad (3)$$

Then these three equations were used for the calculation of the Stokes radii for the native or unfolded proteins with the known molecular weight. Tables I and II contain, in particular, the  $R_S$  values determined in this way.

## RESULTS

**Calibration of Superose-12 Column under Various Solvent Conditions.** To check the dependence of the permeation properties of the Superose-12 column on various solvent systems at 4, 15, and 23 °C, the following experiments were made. First, it was found that the  $V_0$  and  $V_t$  values<sup>2</sup> of the column are practically independent of solution pH, denaturants in wide concentration intervals, and temperature (see Table III).

Second, Figure 2 presents the results of the calibration experiments for the Superose-12 column at 4 °C and 23 °C

<sup>2</sup> Here  $V_0$  is the void volume of the column which is based on the elution volume of blue dextran, and  $V_t$  is the total solvent-accessible column volume, which is based on the elution volume of acetone.

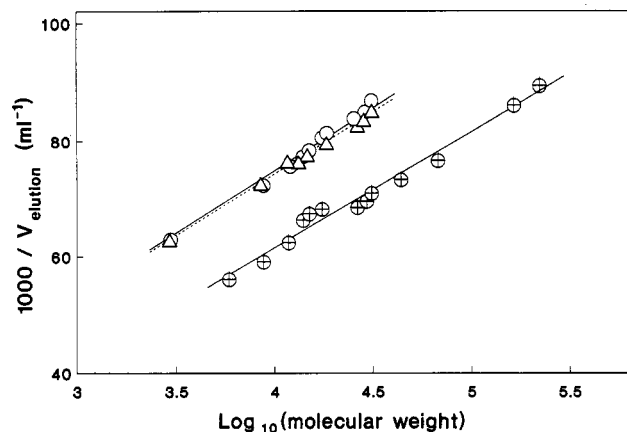


FIGURE 2: Protein molecular weight calibration curves for the Superose-12 column in 0.1 M sodium phosphate, pH 6.8, at 23 °C (●) and in the same buffer containing 6.0 M GdmHCl at 23 °C (○) or 8.0 M urea at 4 °C (Δ).

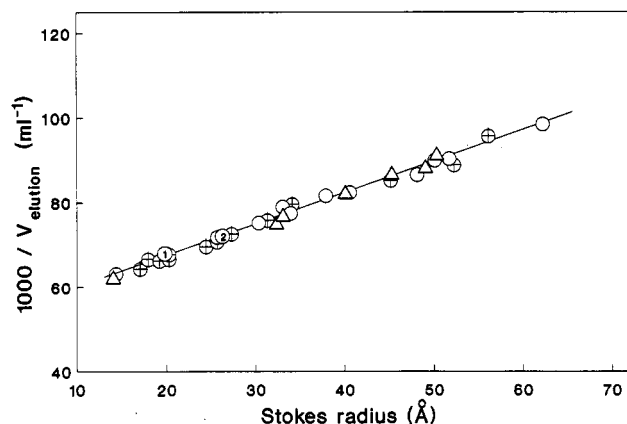


FIGURE 3: Dependence of the migration rate ( $1000/V_{el}$ ) of calibration proteins on their Stokes radius ( $R_s$ ). (●) Data for the native proteins. The results for proteins completely unfolded by GdmHCl or urea are marked with (○) and (Δ), respectively. (one) and (two) show the points corresponding to human  $\alpha$ -lactalbumin and BCAB molten globule states. The Stokes radii were taken from the literature or calculated from eqs 1–3 (Tables I and II).

and in the following solvent systems: 0.1 M sodium phosphate, pH 6.8; 8 M urea, 0.1 M sodium phosphate, 0.01 M DTT, pH 6.8; and 6.0 M GdmHCl, 0.1 M sodium phosphate, 0.01 M DTT, pH 6.8. It is seen that the dependences of the migration rate ( $1000/V_{el}$ ) vs the logarithm of protein molecular weight obtained for different solvents have virtually the same slopes (Figure 2). These data support the conclusion that the permeation properties of the column do not change significantly from 0.1 M sodium phosphate to 6.0 M GdmHCl, 0.1 M sodium phosphate or to 8 M urea, 0.1 M sodium phosphate, pH 6.8.

Figure 3 represents the calibration curve for the Superose-12 column, which permits us to obtain the real parameter of molecular dimensions of proteins. As the permeation properties of our column do not depend on temperature, pH, and denaturant in a wide range of concentration, we have the opportunity to use a simple plot of migration rate ( $1000/V_{el}$ ) vs Stokes radius (Davis, 1983) instead of a more complicated plot of inverse error function complement of partition coefficient<sup>3</sup> ( $K_d$ ) vs Stokes radius as described by Ackers (1967).

<sup>3</sup>  $K_d = (V_x - V_0)/(V_t - V_0)$ , where  $K_d$  is the partition coefficient;  $V_0$  and  $V_t$  are the void and the total solvent accessible column volumes, respectively;  $V_x$  is the elution volume of a given protein under given conditions.

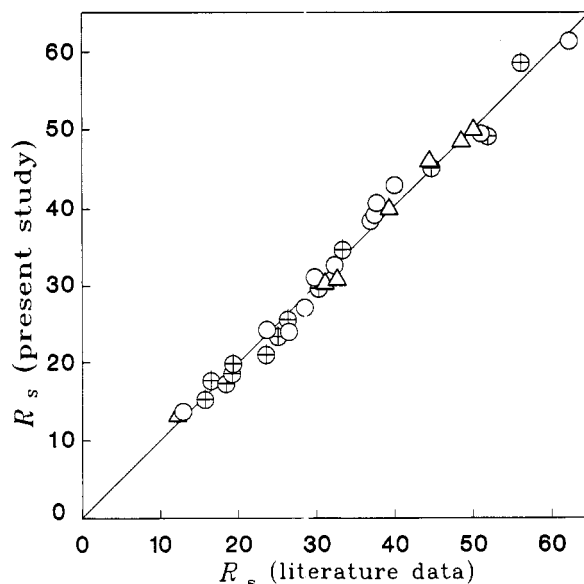


FIGURE 4: Relationship between the values of Stokes radii determined in the present study (from eq 4) and those known from the literature. These results refer to the calibrated proteins in the native state (●) and those completely unfolded by 6 M GdmHCl (○) or by 8 M urea (Δ).

It is seen that all data for the three different solvent conditions [0.1 M sodium phosphate, pH 6.8 (crossed circles); 8 M urea, 0.1 M sodium phosphate, pH 6.8 (triangles); 6.0 M GdmHCl, 0.1 M sodium phosphate, pH 6.8 (circles)] follow the single line shown in Figure 3.

This calibration curve for our Superose-12 column can be described by

$$1000/V_{el} = (0.7247 \pm 0.0003)R_s + (52.1 \pm 0.3) \quad (4)$$

For calibration proteins, it is interesting to compare the  $R_s$  values known from the literature with those calculated from eq 4. The results of the comparison are presented in Figure 4. The Stokes radii determined by FPLC are in good correlation with those known from the literature (Figure 4). This fact indicates that the calibrated SEC column (Superose-12 in our case) can be used to determine the protein molecular dimensions in the native and completely unfolded states.

**Equilibrium of Unfolding Proteins That Unfold in Two-State Manner (Simple  $N \rightleftharpoons U$  Scheme):** *Sperm Whale Myoglobin and Hen Egg White Lysozyme Denaturation by GdmHCl at 4 °C.* The solvent-induced equilibrium unfolding of sperm whale myoglobin and hen egg white lysozyme is well-established. The denaturation transitions of these proteins are the typical "two-state" ones, i.e., their equilibrium unfolding is of the "all-or-none" character (Tanford *et al.*, 1966; Puett, 1973). The Stokes radii of these proteins in the native and unfolded states are known (see Tables I and IV). It has been shown that for the urea-induced unfolding of myoglobin a bimodal distribution on molecular dimensions can be observed by the size-exclusion chromatography (Corbett & Roche, 1984). We have obtained the same results for the GdmHCl-induced unfolding of myoglobin and lysozyme at 4 °C. Figure 5A gives an example of the elution profiles observed for lysozyme at different GdmHCl concentrations: 1, 0; 2, 3.7; 3, 3.9; 4, 4.1; 5, 4.4; 6, 4.7; and 7, 6.2 M. Two elution peaks are observed in the transition area (from 3.7 to 4.7 M GdmHCl). This can be represented as a plot of the retention time for both peaks vs GdmHCl concentration (see insets of Figure 5, panels B and C).

It is interesting that we have observed two well-separated peaks even in the case of lysozyme unfolding (Figure 5, panel

Table IV: Comparison of  $R_S$  Values Determined with Use of FPLC for Different Conformational States of Myoglobin, Lysozyme, Human and Bovine  $\alpha$ -Lactalbumins,  $\beta$ -Lactamase, and Bovine Carbonic Anhydrase with Those Available from Literature

protein	conditions <sup>a</sup>	$R_S^N$	$R_S^M$	$R_S^U$	reference
myoglobin <sup>c</sup>	0.1 M sodium phosphate, pH 6.8, 4 °C	21.4			present study
		20.2			Tanford <i>et al.</i> (1967)
	0.1 M sodium phosphate, 6.0 M GdmHCl, pH 6.8, 4 °C			38.5	present study
				37.8	Ahmad & Salahuddin (1974)
lysozyme <sup>c</sup>	0.1 M sodium phosphate, pH 6.8, 4 °C	19.5			present study
		20.2			Gast <i>et al.</i> (1991)
		18.9			Tanford (1968)
	0.1 M sodium phosphate, 6.0 M GdmHCl, pH 6.8, 4 °C			27.5	present study
				29.3	Gast <i>et al.</i> (1991)
				24.5	Tanford (1968)
	0.1 M sodium phosphate, 6.0 M GdmHCl, 0.01 M DTT, pH 6.8, 4 °C			35.1	present study
				37.5	Gast <i>et al.</i> (1991)
				33.8	Tanford (1968)
	0.1 M sodium phosphate, 8.0 M urea, 0.01 M DTT, pH 6.8, 4 °C			34.5	present study
				33.0	Tanford (1968)
<i>S. aureus</i> $\beta$ -lactamase <sup>d</sup>	0.1 M sodium phosphate, pH 6.8, 23 °C	23.5			present study
	pH 6.8, 23 °C	24.2			from eq 1
	0.1 M sodium phosphate, 6.0 M GdmHCl, pH 6.8, 23 °C			51.6	present study
				49.9	from eq 2
				48.9	from eq 3
bovine $\alpha$ -lactalbumin <sup>d</sup>	0.1 M sodium phosphate, 8.0 M urea, pH 6.8, 23 °C				present study
	0.1 M sodium phosphate, pH 6.8, 4 °C	19.0			Dolgikh <i>et al.</i> (1981)
		19.7			Izume <i>et al.</i> (1983)
		20.1			Bychkova <i>et al.</i> (1990)
		18.4			present study
	0.1 M sodium phosphate, 6.0 M GdmHCl, pH 6.8, 4 °C			25.1	Dolgikh <i>et al.</i> (1981)
				24.1	present study
	0.1 M sodium phosphate, 6.0 M GdmHCl, 0.01 M DTT, pH 6.8, 4 °C			31.8	Izume <i>et al.</i> (1983)
				31.5	Bychkova <i>et al.</i> (1990)
				32.3	present study
human $\alpha$ -lactalbumin	0.1 M sodium phosphate, pH 6.8, 4 °C	18.0			Gast <i>et al.</i> (1991)
		17.7			Gilmanshin <i>et al.</i> (1982)
		19.0			present study
	0.1 M sodium phosphate, 2.0 M GdmHCl, pH 6.8, 4 °C		20.2		Gast <i>et al.</i> (1986)
	0.05 M Tris, <sup>b</sup> 0.01 M EDTA, pH 7.0, 50 °C		19.6		Bychkova <i>et al.</i> (1990)
			19.9		Gast <i>et al.</i> (1991)
	0.1 M sodium phosphate, <sup>b</sup> pH 2.0, 20 °C		19.9		Gilmanshin <i>et al.</i> (1982)
			21.0		Bychkova <i>et al.</i> (1990)
			20.5		present study
	0.1 M sodium phosphate, 6.0 M GdmHCl, pH 6.8, 4 °C			25.8	Gast <i>et al.</i> (1991)
				24.7	Bychkova <i>et al.</i> (1990)
BCAB	0.1 M sodium phosphate, pH 6.8, 15 °C	23.0			present study
		23.6			Wong & Tanford (1973)
		24.5			Rodionova <i>et al.</i> (1989)
	0.1 M sodium phosphate, pH 3.6, 15 °C		25.7		present study
			26.1		Rodionova <i>et al.</i> (1989)
	0.1 M sodium phosphate, 1.6 M GdmHCl, pH 6.8, 15 °C		24.8		present study
	0.1 M sodium phosphate, 6.0 M GdmHCl, pH 6.8, 15 °C			52.1	present study
				51.3	Wong & Tanford (1973)
				50.5	present study
	0.1 M sodium phosphate, 8.0 M urea, pH 6.8, 15 °C			50.1	Rodionova <i>et al.</i> (1989)

<sup>a</sup> Experimental conditions used in the present study (they differ from literature data mainly in temperature). <sup>b</sup> Experimental conditions taken from literature. <sup>c</sup> Proteins whose GdmHCl-induced denaturation is described by a sigmoidal curve (i.e., denatured according to the simple  $N \rightleftharpoons U$  scheme). <sup>d</sup> Proteins that denatured through the molten globule state under an increase of the denaturant concentration (urea or GdmHCl), while their  $N \rightleftharpoons MG$  and  $MG \rightleftharpoons U$  transitions overlap strongly and so they have no "pure" molten globule.

A and panel B, inset). For this protein, the difference in size between the native and the unfolded states with intact disulfide bonds (especially at the beginning of the denaturation transition) is not as large as for myoglobin (see Tables I and IV and Figure 5). This observation can be used as an additional control of the column permeation properties.

FPLC data on protein denaturation can be represented as denaturation curves monitored either by relative areas of the two peaks or, for fast exchange, by the position of the average peak [see, for example, Corbett and Roche (1984)].

Figure 5 represents the results of multiparametric studies of the equilibrium unfolding of lysozyme (Figure 5B) and myoglobin (Figure 5C) by GdmHCl at 4 °C. It is seen that the denaturation curves monitored by the SEC-FPLC coincide with those monitored by far-UV CD and near-UV CD in solution.

*Solvent-Induced Equilibrium Unfolding Proteins That Denature through Molten Globule State: Unfolding of  $\alpha$ -Lactalbumins (at 4 °C), BCAB (at 15 °C), and  $\beta$ -Lactamase (at 23 °C) by GdmHCl- and Urea-Induced Unfolding of  $\beta$ -Lactamase (at 23 °C).* It is known that the molten globule differs from the native state as well as from the fully unfolded one by a higher hydrophobicity (Semisotnov *et al.*, 1991; Ptitsyn, 1992). Thus, the SEC column can be assumed to interact with this intermediate and to affect the equilibrium in the  $N \rightleftharpoons MG \rightleftharpoons U$  denaturation. To verify this assumption, we studied whether the size-exclusion chromatography can be applied to monitor the unfolding of proteins which denature through the molten globule—bovine and human  $\alpha$ -lactalbumins, bovine carbonic anhydrase B, and  $\beta$ -lactamase from *S. aureus*.

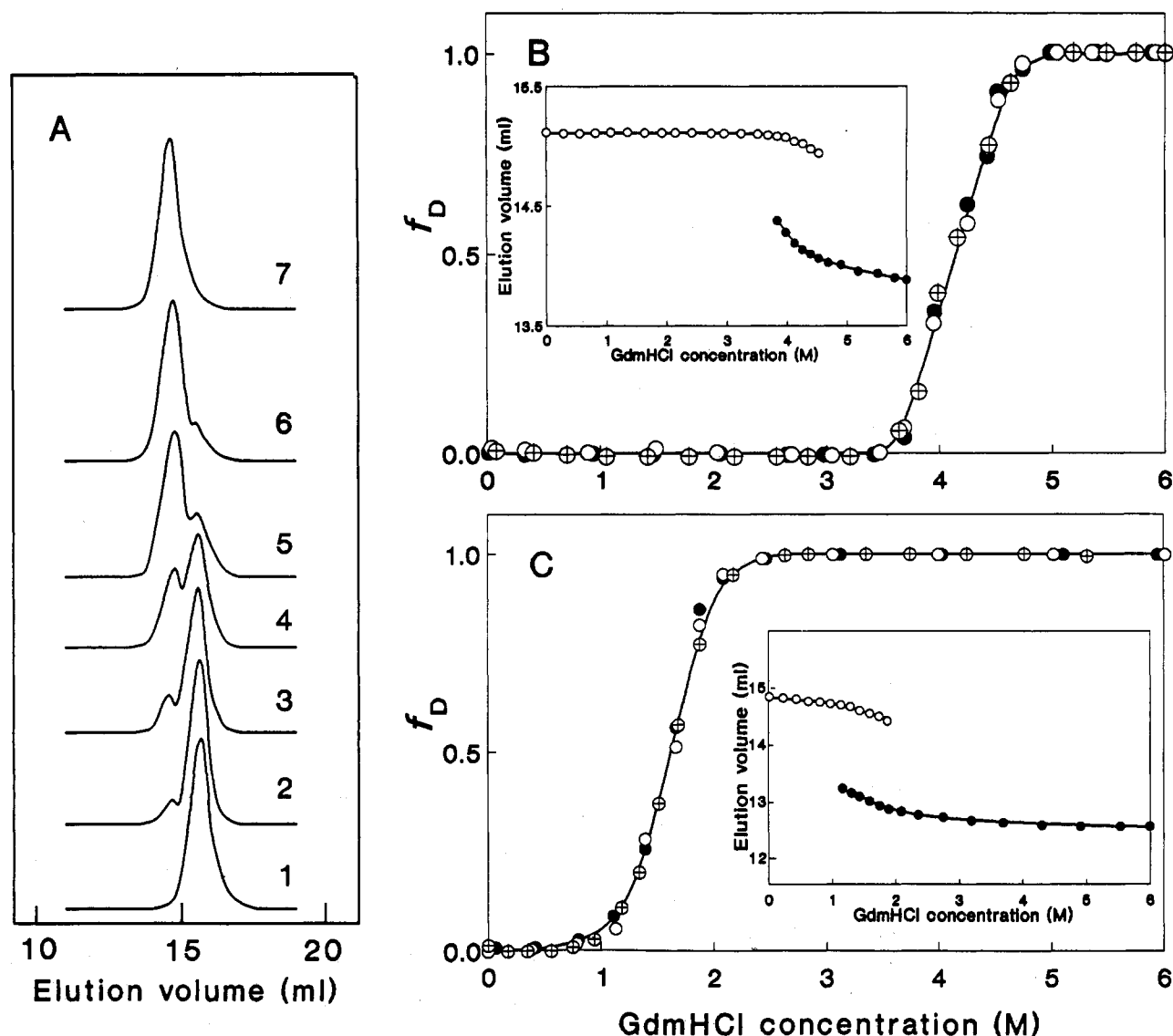


FIGURE 5: Results of multiparametric studies of GdmHCl-induced unfolding of proteins that denature according to the  $N \rightleftharpoons U$  scheme: (A) Elution profiles obtained for the lysozyme within the transition region: 1 corresponds to 0 M GdmHCl; 2, 3.7 M; 3, 3.9 M; 4, 4.1 M; 5, 4.4 M; 6, 4.7 M; and 7, 6.2 M GdmHCl. (B) Comparison of the results obtained for GdmHCl-induced unfolding of the lysozyme by near- (●) and far-UV (○) CD. (●) is the relative area of the FPLC elution peak which corresponds to the unfolded protein molecule. The inset contains the data on GdmHCl dependences of the positions of chromatographic peaks corresponding to the native (○) and unfolded (●) protein molecules. (C) GdmHCl-induced equilibrium unfolding of myoglobin. Decrease of the near- (●) and far-UV (○) CD and increase of the relative area of the elution peak which corresponds to the unfolded protein (●). The inset presents the data on GdmHCl dependences of the positions of size exclusion chromatography elution peaks corresponding to the native and unfolded molecules (○) and (●), respectively. All measurements were made at 4 °C.  $f_D = (X - X_D)/(X_N - X_D)$ , where  $X_N$  and  $X_D$  are the values of the measured parameter for the native and denatured states, respectively.  $X$  refers to the value of this parameter at given conditions.

In GdmHCl-induced unfolding of BCAB (Wong & Tanford, 1973),  $\beta$ -lactamase (Robson & Pain, 1976), and  $\alpha$ -lactalbumins (Kuwaitjima *et al.*, 1976; Nozaka *et al.*, 1978; Dolgikh *et al.*, 1981) as well as in solvent-induced unfolding of many other proteins (Ptitsyn, 1992), the activity and near-UV CD change at smaller GdmHCl concentrations than does the far-UV CD and the hydrodynamic volume of protein molecules. This implies two transitions: the first one is interpreted (Ptitsyn, 1987) as *denaturation* of a protein (i.e.,  $N \rightarrow MG$  transition), and the second one is interpreted as a further *unfolding* of the protein (i.e.,  $MG \rightarrow U$  transition).

As the unfolded molten globule state ( $U \rightarrow MG$ ) transition usually occurs in a few seconds (Ptitsyn *et al.*, 1990; Ptitsyn, 1992), it was not a surprise that, in the cases of urea-induced unfolding of  $\beta$ -lactamase (at 23 °C) and GdmHCl-induced unfolding of BCAB (at 15 °C) and  $\beta$ -lactamase (at 23 °C) or that of bovine and human  $\alpha$ -lactalbumins (at 4 °C), the single elution peak, (which is the average peak) was observed

within the transition region. Figure 6A presents the elution profiles for  $\beta$ -lactamase at different GdmHCl concentrations: 1, 0.00; 2, 0.40; 3, 0.64; 4, 0.80; 5, 0.98; 6, 1.22; 7, 1.51; and 8, 2.22 M. In this case, there is one elution peak which shifts to smaller elution volumes with the increase of GdmHCl concentration. The same situation was observed for BCAB and  $\alpha$ -lactalbumins (data not shown). The denaturation curves followed by FPLC in these cases were monitored by the position of the average peak.

Figure 6 panels B–D present the results of multiparametric investigations of the solvent-induced unfolding of  $\beta$ -lactamase (Figure 6B,C) and bovine  $\alpha$ -lactalbumin (Figure 6D). In all these cases, the two denaturation transitions were observed. This observation is in good agreement with the data reported earlier (Robson & Pain, 1976; Kuwaitjima *et al.*, 1976; Nozaka *et al.*, 1978; Dolgikh *et al.*, 1981). It is necessary to note that the dimension changes monitored by FPLC follow practically the same dependence on the denaturant concentration as the

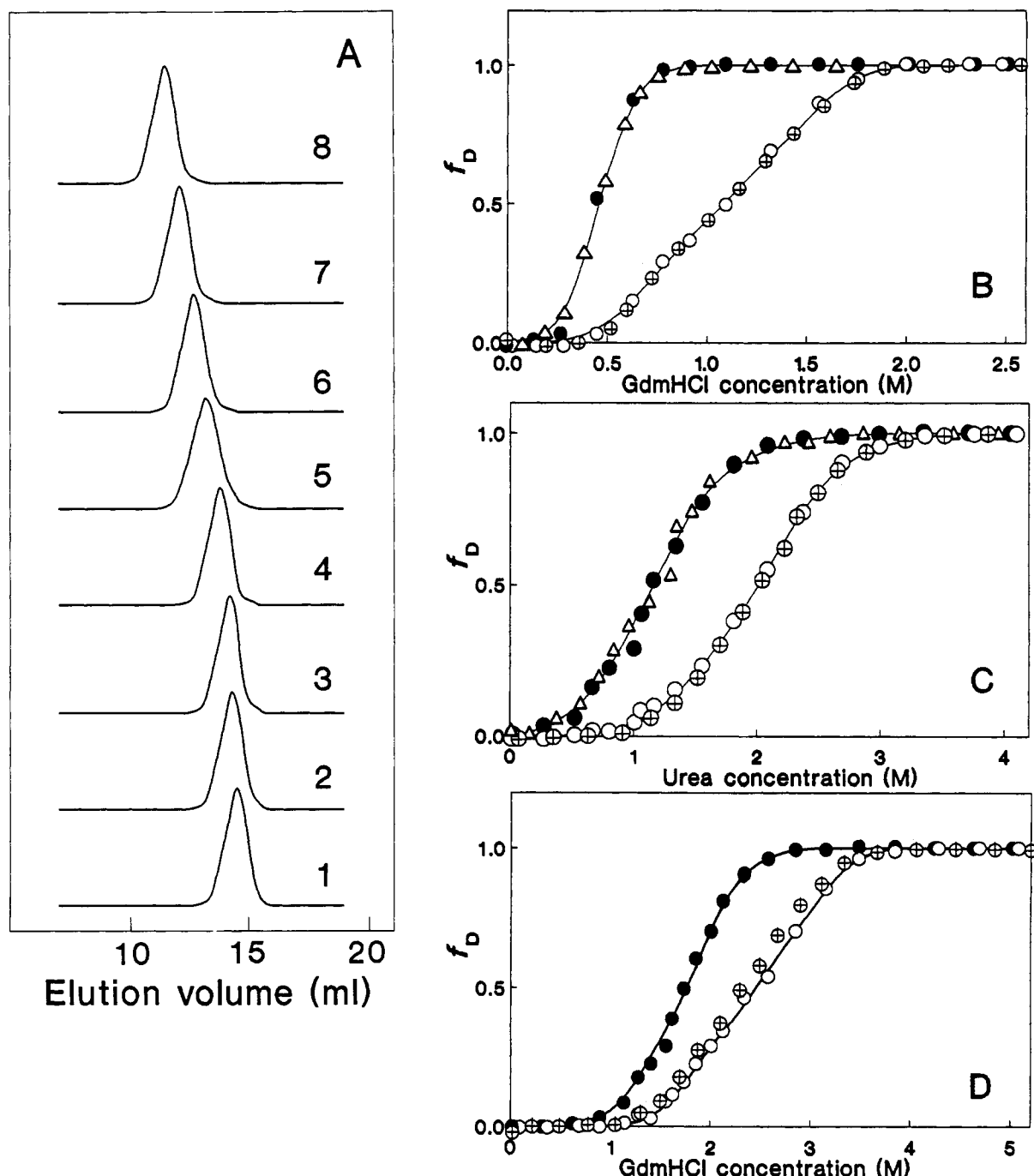


FIGURE 6: Solvent-induced equilibrium unfolding of proteins that denature through the molten globule state. (A) Elution profiles obtained for GdmHCl-induced unfolding of  $\beta$ -lactamase at 4 °C: 1, 0.00; 2, 0.40; 3, 0.64; 4, 0.80; 5, 0.98; 6, 1.22; 7, 1.51; and 8, 2.22 M. (B) GdmHCl-induced unfolding of *Staphylococcus aureus*  $\beta$ -lactamase at 23 °C. Decrease of near-UV CD (molar ellipticity at 270 nm) (●) and far-UV CD (molar ellipticity at 220 nm) (○), decrease of enzymatic activity ( $\Delta$ ) and changes of the position of the average elution peak in FPLC profiles ( $\oplus$ ). The lines describe the best fit of near- and far-UV CD changes. (C) Urea-induced unfolding of *Staphylococcus aureus*  $\beta$ -lactamase at 23 °C. The symbols refer to the same parameters as in panel B. The lines describe the best fit of near- and far-UV CD changes. (D) GdmHCl-induced unfolding of bovine  $\alpha$ -lactalbumin at 4 °C. Decrease of near-UV CD (molar ellipticity at 270 nm) (●) and far-UV CD (molar ellipticity at 220 nm) (○) and changes of the position of the average elution peak in FPLC profiles ( $\oplus$ ). The lines describe the best fit of near- and far-UV CD changes.

decrease of molar ellipticity at 220 nm (see Figure 6B–D).

Figures 7 and 8 present the results of multiparametric studies of the GdmHCl-induced unfolding of human  $\alpha$ -lactalbumin at 4 °C and bovine carbonic anhydrase B at 15 °C, respectively. In these cases, the denaturation curves monitored by FPLC are more complicated than those observed for  $\beta$ -lactamase and bovine  $\alpha$ -lactalbumin (compare Figure 6B–D with Figures 7A and 8A). We can try to deconvolute each of these complicated denaturation curves in two consecutive denaturation processes. It is obvious that such a deconvolution is

not a trivial procedure, especially in the plot presented on Figures 7A and 8A. To simplify a problem of this deconvolution, we have presented the results (Figures 7A and 8A) in the term of a fraction of denatured molecules ( $f_D$ ) that was calculated according to well-known equation:

$$f_D = \frac{V^{\text{el}} - V_N^{\text{el}}}{V_D^{\text{el}} - V_N^{\text{el}}} \quad (5)$$

where  $V^{\text{el}}$  is a value of elution volume at given GdmHCl

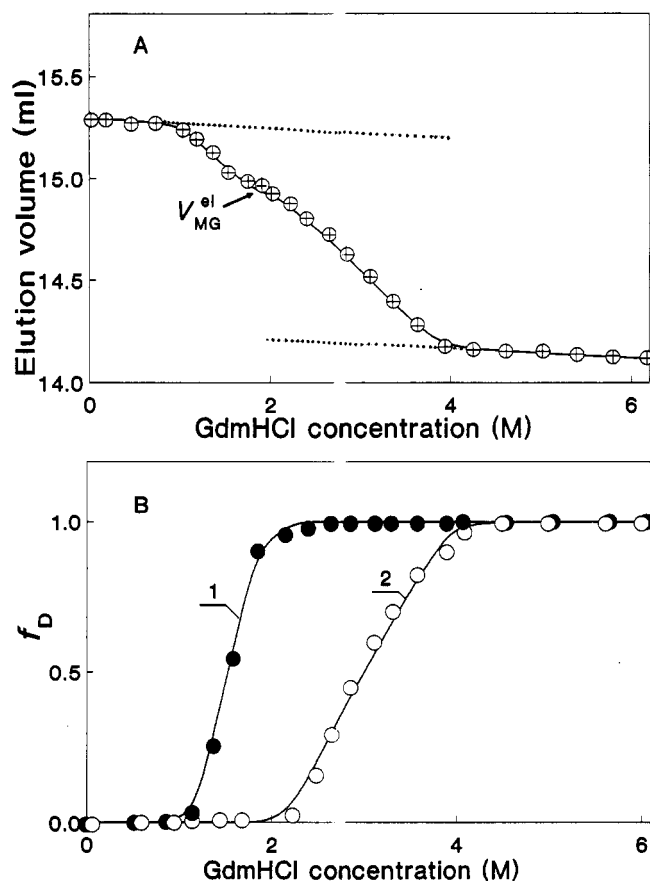


FIGURE 7: GdmHCl-induced equilibrium unfolding of human  $\alpha$ -lactalbumin (at 4 °C). (A) Presents the data on the changes of the position of the average elution peak in FPLC profiles with the increase of GdmHCl concentration ( $\oplus$ ). Baselines are shown by dotted curves. The point used for the calculation of the molten globule dimensions is marked as  $V_{MG}^{el}$ . (B) Summarized results for human  $\alpha$ -lactalbumin unfolding: decrease of CD spectra in the near- ( $\bullet$ ) and far-UV ( $\circ$ ) regions. Curves 1 and 2 result from the deconvolution of the denaturation curve presented in panel A on two denaturation processes (see also Figure 9A). These curves were used for the description of CD changes.

concentration,  $V_N^{el}$  and  $V_D^{el}$  are its values for native and denatured molecules, respectively [which for any GdmHCl concentration were obtained by extrapolation of corresponding baselines (dotted curves on Figures 7A and 8A)]. An example of such presentation for human  $\alpha$ -lactalbumin is shown in Figure 9A. To deconvolute this  $f_D$  vs GdmHCl concentration curve, we have assumed that this complicated denaturation curve consists of two sigmoidal curves which are not overlapped. In this case, the first denaturation transition (indicated as  $N \rightleftharpoons MG$  curve on Figure 9A) coincides with the first stage of  $f_D$  change, while the second one (named  $MG \rightleftharpoons U$  transition) can be obtained by subtracting the sigmoidal  $N \rightleftharpoons MG$  curve from the common dependence of  $f_D$  vs GdmHCl concentration (see Figure 9A).

It is seen that, for human  $\alpha$ -lactalbumin unfolding, the first stage of molecular dimension changes monitored by FPLC takes about 25% of the total effect and indicates the denaturation transition between the native and partly swollen molecules (see Figures 7A and 9A). This denaturation curve describes well the decrease of the near-UV CD spectra (denaturation curve 1, Figure 7B) or, in other words, the  $N \rightleftharpoons MG$  transition. The second stage of  $R_S$  changes (75%) corresponds to the transition from the swollen to the fully unfolded state (see Figure 9A) and describes the changes of intensity of the far-UV CD spectra (Figure 7B, curve 2), i.e., the  $MG \rightleftharpoons U$  transition.

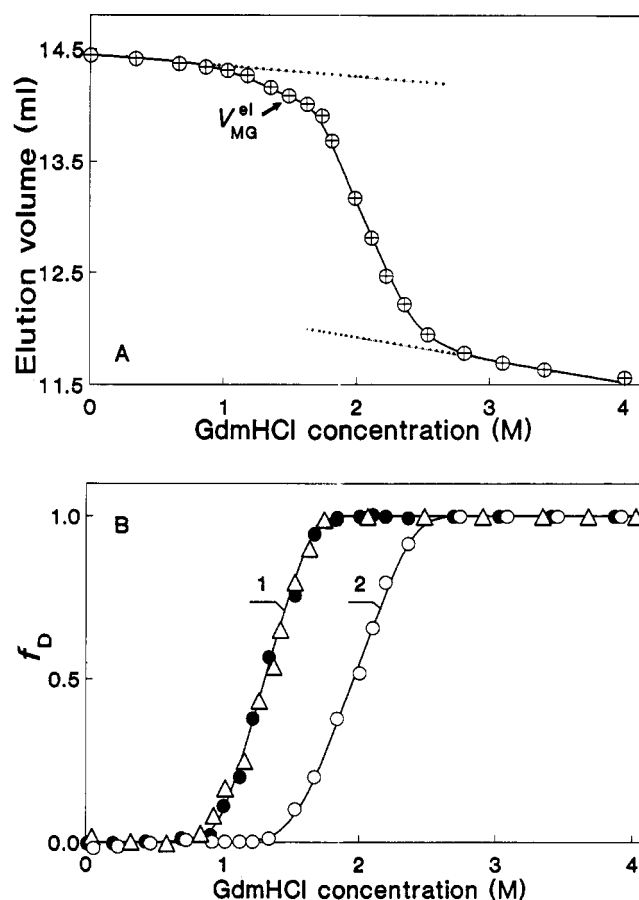


FIGURE 8: GdmHCl-induced equilibrium unfolding of bovine carbonic anhydrase B (at 15 °C). (A) Presents the changes of the position of the average elution peak in FPLC profiles. Baselines are shown by dotted curves. The point used for the calculation of the molten globule dimensions is marked as  $V_{MG}^{el}$ . (B) Data for BCAB unfolding: decrease of the near- ( $\bullet$ ) and far-UV ( $\circ$ ) CD and decrease of protein esterase activity ( $\Delta$ ) with the increase of GdmHCl concentration. Curves 1 and 2 were obtained by deconvolution in the same manner as for human  $\alpha$ -lactalbumin and were used for the description of the changes of CD and esterase activity.

For the BCAB unfolding, the same situation was observed—changes of the position of the average elution peak can be presented as two successive denaturation transitions. The first one separates the compact and slightly more swollen protein molecules, while the second transition corresponds to a further unfolding of this intermediate up to the completely unfolded state (data not shown). As in the case of human  $\alpha$ -lactalbumin unfolding, these two denaturation transitions can be used to describe the changes of CD spectra in terms of the  $N \rightleftharpoons MG \rightleftharpoons U$  unfolding processes (see Figure 8B).

**Use of SEC-FPLC To Estimate Molecular Dimensions of Proteins in Molten Globule State: Human  $\alpha$ -Lactalbumin (2.0 M GdmHCl), BCAB (1.6 M GdmHCl), and BCAB Acid Form (pH 3.6).** Earlier it was shown [see, for example, Corbett and Roche (1984)] that SEC-FPLC can be used to determine the Stokes radii for the native and the unfolded states, and our studies are in good agreement with these data (see Figure 4 and Table IV). The question is to what extent it is correct to use chromatography for the determination of the molecular dimensions of proteins in the molten globule state. To answer this question, we have estimated the  $R_S$  values of different conformational states (N, MG, and U) for proteins whose solvent-induced unfolding can be described by two well-separated (practically not overlapping) denaturation transitions. As shown above (see Figures 6B–D, 7, and 8), the most suitable are the results obtained for the GdmHCl-induced



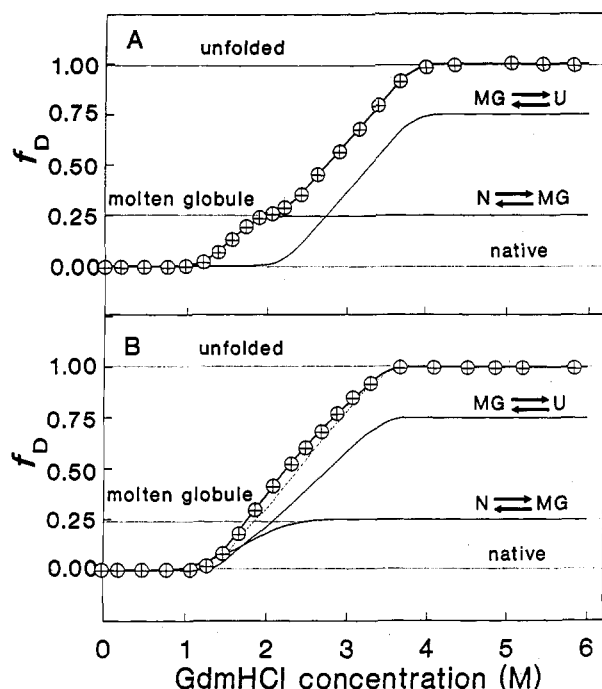


FIGURE 9: Deconvolution of the denaturation curve followed by changes of the position of the average elution peak in FPLC profiles obtained for GdmHCl-induced unfolding of human (A) and bovine (B)  $\alpha$ -lactalbumins at 4 °C. In both cases, the solid line is the sum of two denaturation processes—transitions from the native state to the molten globule and from the molten globule to the completely unfolded state. The curves describing  $N \rightleftharpoons MG$  transitions are those referring to the changes of near-UV CD, while curves for  $MG \rightleftharpoons U$  transitions were taken from changes of far-UV CD. Panel B presents for comparison the curve corresponding to the  $MG \rightleftharpoons U$  transition (---).

denaturation of human  $\alpha$ -lactalbumin and BCAB, and we can estimate the Stokes radius for the different conformational states of these two proteins. The  $R_S$  values in the native and completely unfolded states were calculated by eq 4 using the  $V^{\text{el}}$  values at 0 and 6 M GdmHCl, respectively. To calculate the  $R_S$  values in the molten globule state, we have used the  $V^{\text{el}}$  values corresponding to 1.6 and 2.0 M GdmHCl for BCAB and human  $\alpha$ -lactalbumin, respectively (these points are marked as  $V^{\text{el}}_{\text{MG}}$  on Figures 7A and 8A). The  $R_S$  values in the different conformational states (N, MG, and U) are presented in Table IV. It shows that in both cases the  $N \rightleftharpoons MG$  transition leads to a  $\sim 10\%$  increase of  $R_S$  (from  $\sim 18$  to  $\sim 20$  Å for  $\alpha$ -lactalbumin and from  $\sim 23$  to  $\sim 25$  Å for BCAB, see Table III). The same scale of  $R_S$  changes was observed for the acid form of bovine carbonic anhydrase B, which is a well-known example of the "genuine" molten globule state (Dolgikh *et al.*, 1983; Rodionova *et al.*, 1989; Semisotnov *et al.*, 1991).

## DISCUSSION

The aim of this study was to investigate the suitability of size-exclusion chromatography for monitoring the unfolding of proteins which denature through the molten globule state (according to the  $N \rightleftharpoons MG \rightleftharpoons U$  scheme). For this purpose, we have studied the solvent-induced equilibrium unfolding of sperm whale myoglobin and lysozyme (which denature in a two-state manner), bovine and human  $\alpha$ -lactalbumin, bovine carbonic anhydrase B, and  $\beta$ -lactamase from *S. aureus* (which denature through the molten globule) with the use of activity, circular dichroism, and FPLC.

**What Kind of Information Can Be Obtained by Size-Exclusion Chromatography?** In fact, if the permeation

properties of the given gel-filtration column are known or, in other words, if this column has been calibrated, the SEC-FPLC technique can be used for a simple and fast determination of hydrodynamic volumes of the given protein molecule. If it is known that the column does not affect the equilibrium between the different conformations (N and U, for example), SEC-FPLC can be applied for the monitoring of the changes of molecular dimensions under protein unfolding.

It should be noted that the size-exclusion chromatography provides more than information of integral changes of molecule dimensions under denaturant effect. As a matter of fact, in the case of a slow exchange between different conformers, SEC can show that the function of their distribution on size within the transition region is bimodal. This is one of the sole direct indication of the "all-or-none" mechanism of the solvent-induced unfolding of small globular proteins.<sup>4</sup>

In this case, SEC-FPLC also gives the possibility to observe the native and the denatured states of protein molecules simultaneously and permits checking independent changes of their molecular dimensions. Thus, it opens exceptional possibilities to record individual changes of dimensions of the native and the denatured molecules (instead of an integral description of molecular sizes provided by, e.g., intrinsic viscosity).

**Studies of Permeation Properties of Superose-12 Column in Different Solvent Systems.** We used the traditional calibration procedure to investigate the permeation properties of the Superose-12 column [see, for example, Corbett and Roche (1984)]. We have shown that they do not change significantly from 0.1 M sodium phosphate to 6.0 M GdmHCl, 0.1 M sodium phosphate or to 8 M urea, 0.1 M sodium phosphate, pH 6.8, and do not virtually depend on temperature and pH (see Figures 2 and 3 and Table III). We have also shown that the  $R_S$  values determined for the native and completely unfolded proteins with the use of our calibrated Superose-12 column are in good agreement with the literature data (Figure 4). So, this column may be used for the determination of the Stokes radii of native as well as fully unfolded protein molecules.

**Study of Equilibrium Unfolding of Lysozyme and Myoglobin by GdmHCl.** As an additional control, we have studied the possibility of a column to separate two conformational states (native and unfolded) within the denaturation transition. The GdmHCl-induced unfolding of myoglobin and lysozyme (the proteins denatured in a two-state manner) was studied. It is known that these two proteins have similar dimensions in the native state, while they fully unfolded states have strong differences in sizes (see Tables I and IV). It turned out that the elution peaks corresponding to different conformers are well separated even in the case of lysozyme unfolding (see Figure 5A). What is more, the denaturation curves monitored by FPLC coincide within the experimental error with those followed by near- and far-UV CD changes (Figure 5). This means that the column matrix does not affect either native or fully unfolded states of the proteins and that the Superose-12 column gives correct qualitative information on the protein denaturation process.

The Stokes radii for the native and completely unfolded myoglobin and lysozyme determined with the use of a

<sup>4</sup> It is necessary to emphasize that the same observation was qualitatively made earlier with the use of rapid urea-gradient gel electrophoresis (Creighton, 1980) or with the use of NMR spectroscopy [see, for example, Hardint *et al.* (1991)]. It seems that SEC-FPLC provides much more quantitative information on protein dimensions than the urea-gradient electrophoresis (see below). On the other hand, the experimental procedure for SEC-FPLC is much simpler than that for NMR.

calibrated SEC column are in good correlation with those known from literature (Table IV). This is also true for other proteins used for column calibration (Figure 4). Therefore size-exclusion chromatography can be used not only in qualitative but also in quantitative analysis of the equilibrium unfolding of proteins which denature according to the simple "two-state" model.

**Suitability of SEC-FPLC for Investigations of Unfolding of Proteins That Denature through the Molten Globule State.** Multiparametric studies of the GdmHCl-induced unfolding of bovine and human  $\alpha$ -lactalbumins (at 4 °C), BCAB (at 15 °C), and  $\beta$ -lactamase (at 23 °C) and urea-induced unfolding of  $\beta$ -lactamase (at 23 °C) reveal a similar behavior (see Figures 6 and 7). In all these cases, we observed that the denaturation of proteins occurs in two stages. At the first stage, the intensity of the near-UV CD spectra and biological activity (for BCAB and  $\beta$ -lactamase) decrease (i.e., protein molecules lose their rigid tertiary structure). This corresponds to the N  $\rightleftharpoons$  MG transition (Ptitsyn, 1992). At the second stage [which corresponds to the MG  $\rightarrow$  U transition (Ptitsyn, 1992)], the changes of the elution volume of an average peak in FPLC profiles (or, in other words, the changes of the molecule Stokes radius) follow the same denaturant dependence as the decrease of molar ellipticity at 220 nm. So, we observe simultaneous changes of the protein dimensions and secondary structure under the increase of the denaturant concentration. This indicates that the matrix of the Superose-12 column affects not only N and U but also the intermediate state (MG), and this column can be used for qualitative analysis of the equilibrium unfolding of proteins that denature through the molten globule state.<sup>5</sup>

**Use of SEC-FPLC To Estimate Molecular Dimensions of Proteins in Molten Globule State: Human  $\alpha$ -Lactalbumin (2.0 M GdmHCl), BCAB (1.6 M GdmHCl), and BCAB Acid Form (pH 3.6).** Certainly, the most attractive information that can be obtained with the use of SEC-FPLC is the determination of the molecular dimensions ( $R_s$  values) of protein in different conformers and, particularly, in the molten globule state. It is obvious that the correct  $R_s$  values for the molten globule state can be determined only when the transitions from the native state to the molten globule and from this intermediate to the coil (i.e., N  $\rightleftharpoons$  MG and MG  $\rightleftharpoons$  U transitions) are well-separated. In other words, the molten globule Stokes radius can be determined when a "pure" molten globule exists.

As it follows from our data, the denaturation transitions are well-separated for human  $\alpha$ -lactalbumin (Figure 7B) and BCAB (Figure 8B). As a result, there are two well-defined stages in the changes of the average elution peak position in human  $\alpha$ -lactalbumin (Figure 7A) and BCAB (Figure 8A) unfolding, and the corresponding *two-well separated stages of the molecular dimensions increase*. The first stage reflects the N  $\rightleftharpoons$  MG transition, and the second one reflects the MG  $\rightleftharpoons$  U transition.

In the case of  $\beta$ -lactamase (Figure 6B,C) and bovine  $\alpha$ -lactalbumin (Figure 6D) unfolding, the N  $\rightleftharpoons$  MG and MG  $\rightleftharpoons$  U transitions overlapped. Therefore, the changes of the average elution peak position can be described by a single sigmoidal curve (Figure 6).

To clarify these effects, let us compare the data obtained for human and bovine  $\alpha$ -lactalbumins. As we have already

shown for human  $\alpha$ -lactalbumin (see Figure 7), there is a strong correlation between the stages of molecular dimensions changes and the N  $\rightleftharpoons$  MG and MG  $\rightleftharpoons$  U transitions. For convenience, let us present the results (Figure 7A) as a plot of  $f_D$  vs GdmHCl concentration (Figure 9A). It is obvious that in this dependence line  $f_D = 0$  corresponds to the native state,  $f_D = 0.25$  corresponds to the molten globule state, and  $f_D = 1.0$  corresponds to the completely unfolded state (see Figure 9A).

It is known that acid forms of human and bovine  $\alpha$ -lactalbumins have similar scales of the swell in comparison with the molecular dimensions of their native states (Ptitsyn, 1992). Thus, we can assume that the molten globules observed for these proteins at mild GdmHCl concentrations have a comparable scale of the swell too. If this is correct, in bovine  $\alpha$ -lactalbumin unfolding by GdmHCl the N  $\rightleftharpoons$  MG transition accounts for  $\sim 25\%$  of the common effect of molecular dimensions increase, and the remaining 75% reflect the MG  $\rightleftharpoons$  U transition (Figure 9B). The curves corresponding to N  $\rightleftharpoons$  MG and MG  $\rightleftharpoons$  U transitions were taken from Figure 6D (they describe changes of bovine  $\alpha$ -lactalbumin CD spectra in the near- and far-UV regions) with the respective coefficients (0.25 for the near- and 0.75 for far-UV CD). As follows from Figure 9B, the data obtained for GdmHCl-induced changes of the molecular dimensions of bovine  $\alpha$ -lactalbumin can be well-described by a sigmoidal curve which is a simple sum of the curves corresponding to N  $\rightleftharpoons$  MG and MG  $\rightleftharpoons$  U transitions (see Figure 9B). A large overlapping of these transitions leads to a practically complete coincidence of the curve corresponding to the MG  $\rightleftharpoons$  U transition with the overall curve (see Figure 9B).

BCAB is known to transfer to the molten globule state not only at a mild GdmHCl concentration but also at acid pH values (pH 3.6; Dolgikh *et al.*, 1983) and this "acid" form of BCAB is an example of the so-called "pure" molten globule state (Dolgikh *et al.*, 1983; Rodionova *et al.*, 1989; Semisotnov *et al.*, 1991). We can also determine the dimensions of the BCAB molten globule at pH 3.6, and Table IV gives the Stokes radius obtained for this acid form. It is seen that the dimensions of the BCAB molecule in the molten globule state (1.6 M GdmHCl) and in the acid form (pH 3.6) are practically the same ( $R_s = 24.8$  and  $25.7$  Å, respectively), which corresponds to comparable scales of the protein molecule swell (the molecular volume increases 1.25 times in the first case and 1.40 times in the second).

It is worth emphasizing that our results on  $R_s$  are in good correlation with literature data (see Table IV). The coincidence of the Stokes radius of the molten globule obtained by laser-light scattering (Gast *et al.*, 1991), by macroscopic diffusion with polarization optics (Bychkova *et al.*, 1990), as calculated from intrinsic viscosity (Gilmanshin *et al.*, 1982; Rodionova *et al.*, 1989), and by FPLC (this paper) indicates that SEC-FPLC is suitable for quantitative studies of equilibrium unfolding of proteins that denature through the molten globule.

Thus, size-exclusion fast protein liquid chromatography is an "inert" technique, i.e., it does not shift the equilibrium between the N, MG, and U states and, therefore, not only can be used for a quantitative study of solvent-induced unfolding of proteins that denature according to the "two-state" model but also can be applied to determine denaturant-induced changes of the dimensions of protein molecules that denature on the N  $\rightleftharpoons$  MG  $\rightleftharpoons$  U denaturation scheme.

<sup>5</sup> The direct evidence of this suggestion has been obtained earlier. The comparison of the denaturation curve reflected the protein activity decrease in solution with the same dependence as that observed for protein just after it was released from the gel filtration column (Uversky *et al.*, 1992).

## ACKNOWLEDGMENT

I am grateful to Profs. O. B. Ptitsyn and A. V. Finkelstein and Drs. G. V. Semisotnov, D. E. Bochkariov, and N. M. Lissin for valuable and useful discussions and to Prof. O. B. Ptitsyn for reading the manuscript and making important comments. I thank Dr. N. V. Kotova for the sample of BCAB, Dr. T. Picard for the sample of  $\beta$ -lactamase, and Drs. N. V. Kotova and V. E. Bychkova for the samples of bovine and human  $\alpha$ -lactalbumins and bovine  $\beta$ -lactoglobulin.

## REFERENCES

- Ackers, G. L. (1967) *J. Biol. Chem.* **242**, 3237.  
 Ackers, G. L. (1970) *Adv. Protein Chem.* **24**, 343.  
 Ahmad, F., & Salahuddin, A. (1974) *Biochemistry* **13**, 245.  
 Armstrong, J. McD., Myers, D. V., Verpoorte, J. A., & Eddsall, J. T. (1966) *J. Biol. Chem.* **241**, 5137.  
 Brems, D. N., Plaisted, S. M., Havel, H. S., Kauffman, E. W., Stodola, J. D., Eaton, L. C., & White, R. D. (1985) *Biochemistry* **24**, 7662.  
 Bychkova, V. E., Bartoshevich, S. F., & Klenin, S. L. (1990) *Biofizika* **35**, 242.  
 Calam, D. H., & Davidson, J. (1981) *J. Chromatogr.* **218**, 581.  
 Castellino, F. J., & Barker, R. (1968) *Biochemistry* **7**, 2207.  
 Corbett, R. J. T., & Roche, R. S. (1983) *Dev. Biochem.* **25**, 79.  
 Corbett, R. J. T., & Roche, R. S. (1984) *Biochemistry* **23**, 1888.  
 Creighton, T. E. (1980) *J. Mol. Biol.* **137**, 61.  
 Davis, L. C. (1983) *Chromatogr. Sci.* **21**, 214.  
 DeCrombrughe, B., Pitt-Rivers, R., & Edelhoch, H. (1966) *J. Biol. Chem.* **241**, 2766.  
 Dolgikh, D. A., Gilmanshin, R. I., Braznikov, E. V., Bychkova, V. E., Semisotnov, G. V., Venyaminov, S. Yu., & Ptitsyn, O. B. (1981) *FEBS Lett.* **136**, 311.  
 Dolgikh, D. A., Abaturov, L. V., Braznikov, E. V., Lebedev, O. Yu., Chirgadze, Yu. N., & Ptitsyn, O. B. (1983) *Dokl. Akad. Nauk SSSR* **272**, 1481.  
 Dubin, S. B., Feher, G., & Benedek, G. B. (1973) *Biochemistry* **12**, 714.  
 Endo, S., Saito, Y., & Wada, A. (1983) *Anal. Biochem.* **131**, 108.  
 Fish, W. S., Reynolds, J. A., & Tanford, C. (1970) *J. Biol. Chem.* **245**, 5166.  
 Gast, K., Zirwer, D., Welfe, H., Bychkova, V. E., & Ptitsyn, O. B. (1986) *Int. J. Biol. Macromol.* **8**, 231.  
 Gast, K., Damashun, G., Damashun, H., Misselwitz, R., Zirwer, D., & Bychkova, V. E. (1991) in *Laser Light Scattering in Biochemistry* (Harding, S., & Sattelle, D. B., Eds.) p 209, Thomas Graham House, Cambridge, U.K.  
 Gilmanshin, R. I., Dolgikh, D. A., Ptitsyn, O. B., Finkelstein, A. V., & Shakhnovich, E. I. (1982) *Biofizika* **27**, 1005.  
 Gupta, B. B. (1983) *J. Chromatogr.* **282**, 463.  
 Harding, M. M., Williams, D. H., & Wolfson, D. N. (1984) *Biochemistry* **30**, 3120.  
 Harrington, W. F., & Karr, G. M. (1965) *J. Mol. Biol.* **13**, 885.  
 Houghlum, J. E., & Chappel, G. S. (1984) *J. Liq. Chromatogr.* **7**, 2895.  
 Ingham, K. C., Busby, T. F., Atha, D. H., & Forastieri, H. (1983) *J. Liq. Chromatogr.* **6**, 229.  
 Izumi, Y., Miyake, Y., Kuwajima, K., Sugai, S., Inoue, K., Izumi, M., & Katano, S. (1983) *Physica* **120B**, 444.  
 Janson, J. A. (1965) *Biochim. Biophys. Acta* **99**, 171.  
 Kuwajima, Nitta, K., Yoneyama, M., & Sugai, S. (1976) *J. Mol. Biol.* **106**, 359.  
 Lapanje, S. (1969) *Croat. Chem. Acta* **41**, 115.  
 Lau, S. Y. M., Taneja, A. K., & Hodges, R. S. (1984) *J. Chromatogr.* **246**, 129.  
 LeMaire, M., Rivas, E., & Muller, J. V. (1980) *Anal. Biochem.* **106**, 12.  
 Nozaka, M., Kuwajima, K., Nitta, K., & Sugai, S. (1978) *Biochemistry* **17**, 3753.  
 Privalov, P. L. (1979) *Adv. Protein Chem.* **33**, 167.  
 Ptitsyn, O. B. (1987) *J. Protein Chem.* **6**, 273.  
 Ptitsyn, O. B. (1992) in *Protein Folding* (Creighton, T. E., Ed.) Vol. 4, p 245, W. H. Freeman & Co., New York.  
 Ptitsyn, O. B., Pain, R. H., Semisotnov, G. V., Zerovnik, E., & Razgulyaev, O. I. (1990) *FEBS Lett.* **262**, 20.  
 Puett, D. (1973) *J. Biol. Chem.* **248**, 4623.  
 Robson, B., & Pain, R. H. (1976) *Biochem. J.* **155**, 331.  
 Robson, B., & Pain, R. H. (1976) *Biochem. J.* **155**, 331.  
 Rodionova, N. A., Semisotnov, G. V., Kutysenko, V. P., Uversky, V. N., Bolotina, I. A., Bychkova, V. E., & Ptitsyn, O. B. (1989) *Mol. Biol.* **23**, 683.  
 Semisotnov, G. V., Rodionova, N. A., Razulyaev, O. I., Uversky, V. N., Gripas, A. F., & Gilmanshin, R. I. (1991) *Biopolymers* **31**, 119.  
 Tanford, C. (1968) *Adv. Protein Chem.* **23**, 122.  
 Tanford, C. (1970) *Adv. Protein Chem.* **24**, 1.  
 Tanford, C., Pain, R. H., & Otchin, N. S. (1966) *J. Mol. Biol.* **15**, 489.  
 Tandord, C., Kawahara, K., & Lapanje, S. (1967) *J. Am. Chem. Soc.* **89**, 729.  
 Uversky, V. N., Semisotnov, G. V., Pain, R. H., & Ptitsyn, O. B. (1992) *FEBS Lett.* **314**, 89.  
 Voll, M. J., Appella, E., & Martin, R. G. (1967) *J. Biol. Chem.* **242**, 1760.  
 Withka, J., Moncuse, P., Baziotis, A., & Maskiewicz, R. (1987) *J. Chromatogr.* **398**, 175.  
 Wong, K.-P., & Tanford, C. (1973) *J. Biol. Chem.* **248**, 8518.